Article:
Rodriguez Zaurin, J., Tadhunter, C.N. and Gonzalez Delgado, R.M. (2008) Optical spectroscopy of Arp220: the star formation history of the closest ULIRG. Monthly Notices of the Royal Astronomical Society, 384 (3). pp. 875-885. ISSN: 0035-8711

https://doi.org/10.1111/j.1365-2966.2007.12658.x

Mon. Not. R. Astron. Soc. **384,** 875–885 (2008) doi:10.1111/j.1365-2966.2007.12658.x

Optical spectroscopy of Arp220: the star formation history of the closest ULIRG

J. Rodríguez Zaurín,[1⋆] C. N. Tadhunter[1] and R. M. González Delgado[2]

[1]*Department of physics and Astronomy, University of Sheffield, Sheffield S3 7RH*
[2]*Instituto de Astrofisica de Andalucia (CSIC), P. O. Box 3004, 18080 Granada, Spain*

Accepted 2007 October 31. Received 2007 October 31; in original form 2007 August 6

ABSTRACT

We present long-slit, optical spectra of the merging system Arp220, obtained using the William Herschel Telescope (WHT) on La Palma. These data were taken as a part of a large study of ultraluminous infrared galaxies (ULIRGs) with the aim of investigating the evolution and star formation histories of such objects. Spectral synthesis modelling has been used to estimate the ages of the stellar populations found in the diffuse light sampled by the spectra. As the closest ULIRG, it proved possible to perform a detailed study of the stellar populations over the entire body of the object. The data show a remarkable uniformity in the stellar populations across the full 65 arcsec covered by our slit positions, sampling the measurable extent of the galaxy. The results are consistent with a dominant intermediate-age stellar population (ISP) with age $0.5 \leqslant t_{\rm ISP} \leqslant 0.9$ Gyr that is present at all locations, with varying contributions from a young ($\leqslant$0.1 Gyr) stellar population (YSP) component. However, it is notable that while the flux contribution of the YSP component in the extended regions is relatively small ($\leqslant$40 per cent), adequate fits in the nuclear region are only found for combinations with a significant contribution of a YSP component (22–63 per cent). Moreover, while a low intrinsic reddening ($E(B-V) \lesssim 0.3$) is found for the ISPs in the extended regions, intrinsic reddening values as high as $E(B-V) \sim 1.0$ are required in the galactic centre. This clearly reflects the presence of a reddening gradient, with higher concentrations of gas and dust towards the nuclear regions, coinciding with dust lanes in the *Hubble Space Telescope* images. Overall, our results are consistent with models that predict an epoch of enhanced star formation coinciding with the first pass of the merging nuclei (represented by the ISP), with a further episode of star formation occurring as the nuclei finally merge together (represented by the YSP and ULIRG).

Key words: galaxies: evolution – galaxies: individual: Arp220 – galaxies: starburst.

1 INTRODUCTION

Since the early 1980s, several studies have revealed the presence of galaxies with spectral energy distributions (SEDs) dominated by infrared (IR) emission (Houck et al. 1984; Soifer et al. 1984a,b; Houck et al. 1985; Soifer et al. 1987; Le Floc'h et al. 2005). These galaxies are classified as luminous ($L_{\rm ir} > 10^{11}\,{\rm L}_{\odot}$) or ultraluminous ($L_{\rm ir} > 10^{12}\,{\rm L}_{\odot}$) IR galaxies (LIRGs/ULIRGs). Their prodigious IR emission is generally attributed to the optical/UV light of luminous central sources reprocessed by dust. Starburst activity is ongoing in most, if not all, of these sources, coexisting with active galactic nucleus (AGN) activity in some cases (Genzel et al. 1998; Surace & Sanders 1999; Veilleux, Sanders & Kim 1999). Therefore these objects provide us with an excellent opportunity to study both AGN and starburst phenomena. Moreover ULIRGs are almost unvariably associated with galaxy mergers and interactions (see Sanders & Mirabel 1996 for a revision). Thus, they also represent ideal objects to test models of galaxy evolution via major galaxy mergers (e.g. Barnes & Hernquist 1996; Mihos & Hernquist 1996; Springel, Di Mateo & Hernquist 2005).

In this context Arp220, as the closest ULIRG ($z = 0.018$), is a key object for our understanding of star formation in galaxy mergers. At IR wavelengths, it appears as a double nucleus system (Graham et al. 1990; Scoville et al. 1998) separated 0.95 arcsec, with two tidal tails visible at optical wavelengths (Joseph & Wright 1985). Although the mid-IR spectra suggest starburst activity as the main source of power for the IR continuum (Genzel et al. 1998; Lutz, Veilluex & Genzel 1999), the galaxy is classified as a LINER in the optical (Veilleux et al. 1999). Arp220 was also observed by

⋆E-mail: jrzaurin@sheffield.ac.uk

Scoville, Yun & Bryant (1997) at 1.3 and 2.6 μm, sampling the CO (2–1), CO (1–0) and dust continuum emission. They determine a total H_2 mass of $3.2 \times 10^{10}\,M_\odot$, of which 2/3 is contained within 250 pc and confined to a thin, centrally located, dense disc, embedded in a CO disc extended by ∼1 kpc. The dynamics of the nuclear region are consistent with a collision between prograde and retrograde discs overlapping with the main gas disc (Mundell, Ferruit & Pedlar 2001, see fig. 7 in their paper). Recently, Wilson et al. (2006) performed a detailed photometric study of the star clusters in Arp220. They found evidence that the cluster population can be divided into two groups: a centrally located young population of age $t_{\rm YSP} \lesssim 10$ Myr, and an intermediate-age population of age ∼300 Myr spread towards the north of the galaxy. However, given the photometric uncertainties, it is not straightforward to break the age/reddening degeneracy problem unambiguously in such studies, based only on colour–colour diagrams with relatively few filters.

To date, there have been few spectroscopic studies of stellar populations in ULIRGs. To remedy this situation we present in this paper a detailed study of the stellar populations in Arp220, based on spectroscopic observations of the extended diffuse light along three slit positions. The results are discussed in the context of evolutionary models of star formation in mergers.

Throughout the paper we assume $H_0 = 71\,{\rm km\,s^{-1}}$, $\Omega_0 = 0.27$ and $\Omega_\Lambda = 0.73$, resulting in a scale of 0.363 kpc arcsec^{-1} and a distance of 77.6 Mpc at $z = 0.018$.

2 OBSERVATIONS AND DATA REDUCTION

Spectra of Arp220 were taken in 2005 July and 2006 July with the ISIS dual-beam spectrograph on the 4.2-m William Herschel Telescope (WHT) on La Palma. The R300B grating with the EEV12 CCD, and R316R grating with MARCONI2 CCD were used on the blue and the red arms, respectively. A dichroic cutting at 5300 Å was used during the observations, leading to a useful wavelength range in the rest frame of 3000–5000 Å in the blue, and 5000–7800 Å in the red. The spectra were taken along three slit positions: PA 160, PA 75 and PA 75* (10 arsec offset to the north of PA 75), covering the nuclear region and also the tidal tail observed towards the north-west of the galaxy. Details of the observations are given in Table 1. Fig. 1 shows the slit positions superimposed on *Hubble Space Telescope* (*HST*) images taken with the WFPC2 (HST proposal 6346, PI K. Borne) and the ACS HRC (HST proposal 9396, PI C. Wilson) cameras. To find the precise locations of the slits on the images we first convolved the images with Gaussian profiles to simulate the seeing conditions during our WHT observations. Several spatial profiles were then extracted from the images and compared with those of spatial slices extracted from the spectra using a wavelength range as close as possible to that of the images, until a match was found. All exposures were taken with the slit aligned along the parallactic angle, in order to minimize the effects of the differential refraction.

Table 1. Summary of the spectroscopic observations of Arp220.

Date	Arm	Set-up (CCD + grating)	Slit PA	Slit width (arcsec)	Exposure time (s)	Seeing (arcsec)
2005 July	B	EEV12 + R300B	160	1.5	900	1.85
2005 July	R	MARCONI2 + R316R	160	1.5	900	1.85
2006 July	B	EEV12 + R300B	75	1.5	900	0.65
2006 July	R	MARCONI2 + R316R	75	1.5	900	0.65
2006 July	B	EEV12 + R300B	75*	1.5	1200	0.75
2006 July	R	MARCONI2 + R316R	75*	1.5	1200	0.75

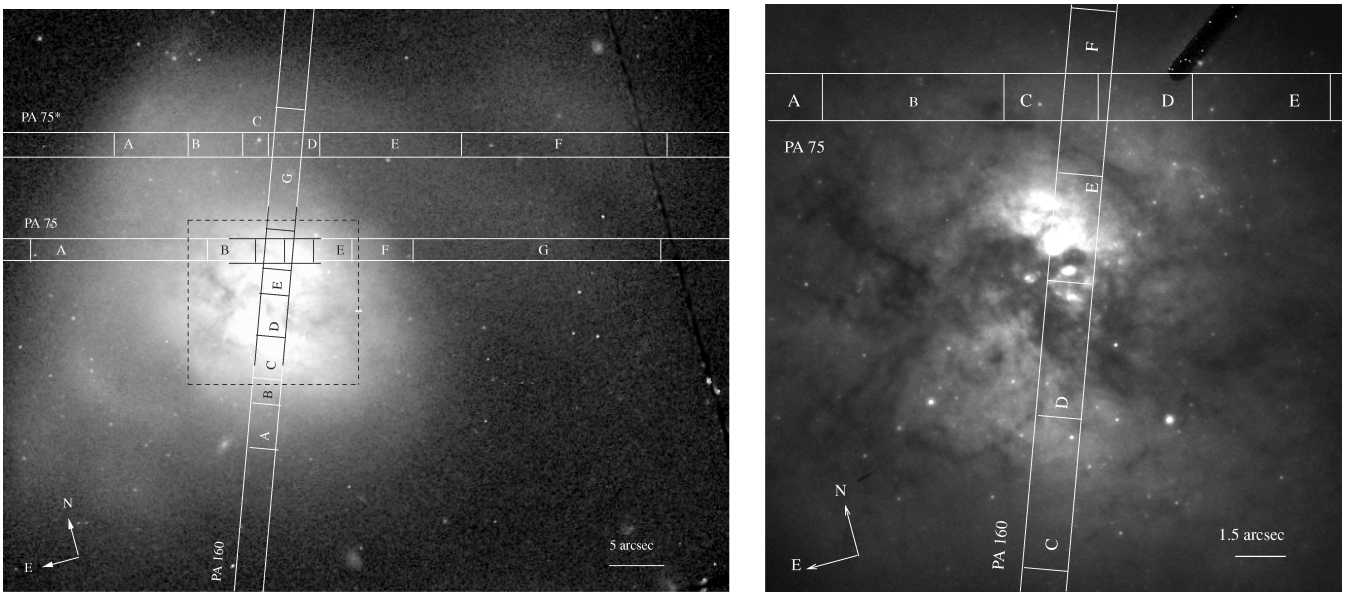

Figure 1. *HST* images taken with the F814W filter, showing the locations of the slits and the extraction apertures. Left-hand panel: WFPC2 image showing both the nuclear region and the extended regions. Right-hand panel: ACS HRC Image showing the region within the dashed-line box in the left-hand panel.

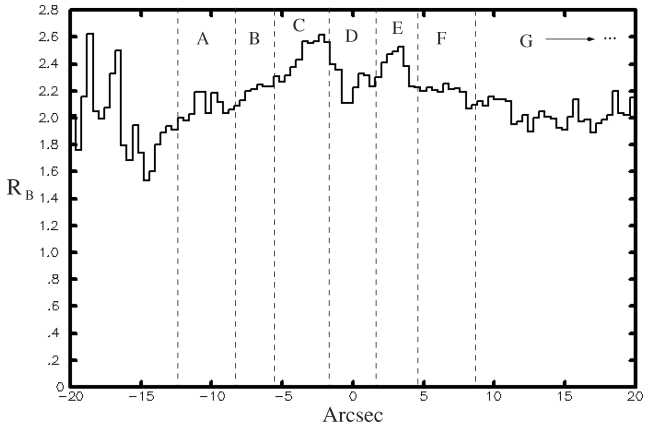

Figure 2. The Balmer break ratio R_B plotted as a function of position along PA 160. The small variations of the ratio suggest a remarkable uniformity for the stellar populations along the extension covered by the slit position. The centroid of Ap D is used as the reference point. Positive *x*-axis: north, negative *x*-axis: south.

The data were reduced (bias subtraction, flat-field correction, cosmic ray removal, wavelength calibration and flux calibration) and straightened before the extraction of the individual spectra using the standard packages in IRAF and the STARLINK packages FIGARO and DIPSO. The wavelength calibration accuracy, calculated as the mean value of the difference between the published (Osterbrock et al. 1996) and the measured wavelengths of the night sky lines was estimated as <0.34 Å and <0.45 Å in the blue and the red, respectively. The spectral resolution, calculated as the mean value of the sky line width (FWHM) was 5.80 Å in the blue and 5.25 Å in the red. The relative flux calibration accuracy, based on the observation of several spectrophotometric standard stars, was estimated as ± 5 per cent over the entire spectral range. This is confirmed by the excellent match between the blue and the red spectra for all the apertures extracted. Prior to the modelling, the spectra were corrected for Galactic extinction using the Seaton (1979) reddening law and the value of $E(B-V) = 0.051$ from Schlegel, Finkbeiner & Davis (1998).

3 RESULTS

In order to gain a preliminary impression of the variations of the stellar populations, in Fig. 2 we plot the flux ratio,

$$R_{\rm B} = \frac{\int_{4000}^{4080} F_\lambda {\rm d}\lambda}{\int_{3620}^{3700} F_\lambda {\rm d}\lambda}, \quad (1)$$

as a function of position along PA 160. This ratio, which is designed to provide a sensitive measure of the Balmer break, shows remarkably little variation across the galaxy (typical variation ± 10 per cent) except in the region of the nucleus (within ± 5 arcsec of the centre) which is subject to enhanced reddening.

To further investigate the stellar populations, 20 apertures were extracted along the three slit positions with the aim of adequately sampling the different regions observed in both the 2D spectra and the available *HST* images. These apertures are labelled in Fig. 1. Three larger apertures, including all the small apertures for each slit PA, were also extracted. The latter are labelled as AP_{TOTAL} in Fig. 3 and Tables 2 and 3. The apertures extracted for the three slit positions are shown superimposed on spatial profiles of the 2D spectra for the wavelength range 4400–4600 Å in Fig. 3. The apertures were chosen to be wide enough to have a sufficiently high signal-to-noise

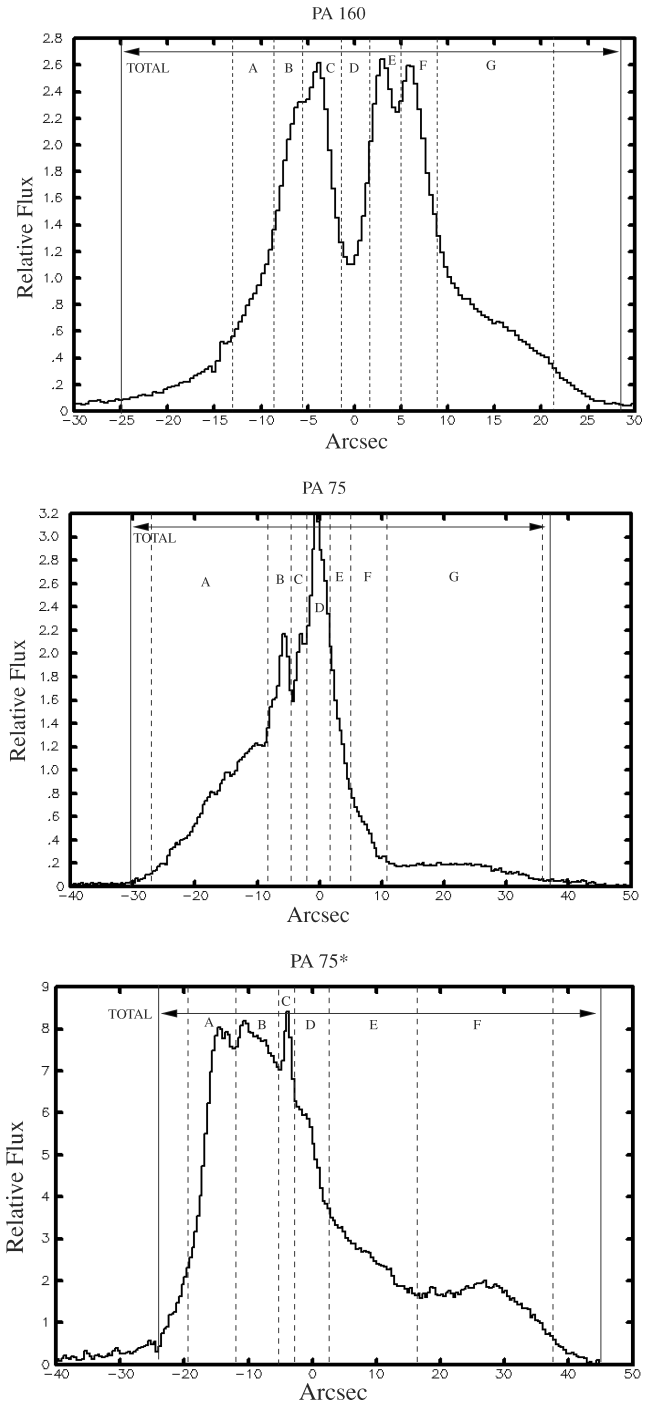

Figure 3. Spatial profiles of the 2D spectra for the wavelength range 4400–4600 Å showing the positions of the extraction apertures. The centroid of Ap D is chosen as the reference point for the three slit positions, PA 160, PA 75 and PA 75*. PA 160: positive *x*-axis: north, negative *x*-axis: south. PA 75 and PA 75*: positive *x*-axis: west, negative *x*-axis: east.

ratio (S/N) for further analysis: S/N > 15. We would like to emphasize that the S/N is considerably higher than this for most of the apertures extracted from the different regions of the galaxy. A sample of extracted spectra is shown in Fig. 4. The strong Balmer lines and Balmer break present across the full measurable extent of the galaxy (65 arcsec) indicate that young (YSPs) and/or intermediate-age stellar populations (ISPs) are present in all spatial apertures. The

Table 2. Modelling results obtained using the STARLIGHT code with the González Delgado et al. (2005) synthetic SEDs. Column 1: slit PA. Column 2: aperture label. Apertures D and E from PA 160 sample the nuclear regions of the galaxy. Column 3: width of the aperture (the centroid of Ap D is chosen to be the reference point for all the slit positions). Column 4: the intrinsic reddening value obtained for the best-fitting models assuming the same extinction for all the stellar components. Columns 5–7: the flux percentage at 4020 Å of each population, as defined in Section 3.

(1)	(2)	Width of the aperture (arcsec) (3)	$E(B-V)$ (4)	%YSP (5)	%ISP (6)	%OSP (7)
PA 160	Ap A	−12.6 to −8.2	0.0	0	112	0
	Ap B	−8.2 to −5.4	0.1	0	109	0
	Ap C	−5.4 to −1.8	0.4	10	96	0
	Ap D	−1.8 to 1.8	0.8	58	34	9
	Ap E	1.8–4.6	0.7	35	63	5
	Ap F	4.6–8.6	0.4	30	71	2
	Ap G	8.6–22.6	0.2	13	91	0
	AP_{TOTAL}	−24.4 to 28.4	0	25	80	1
PA 75	Ap A	−26.6 to −8.6	0.3	10	96	0
	Ap B	−8.6 to −4.2	0.5	33	68	2
	Ap C	−4.2 to −1.4	0.5	25	77	2
	Ap D	−1.4 to 1.4	0.4	16	88	0
	Ap E	1.4–5.0	0.4	21	84	1
	Ap F	5.0–10.2	0.4	15	87	0
	Ap G	10.2–34.6	0.3	21	91	0
	AP_{TOTAL}	−29.4 to 35.8	0.4	18	87	0
PA75*	Ap A	−19.2 to −12.0	0.2	16	89	0
	Ap B	−12.0 to 5.2	0.2	9	96	0
	Ap C	−5.2 to −2.8	0.2	15	89	0
	Ap D	−2.8 to 2.8	0.2	16	90	0
	Ap E	2.8–17.6	0.2	17	91	0
	Ap F	17.6–38.4	0.2	14	93	0
	AP_{TOTAL}	−23.2 to 45.6	0	14	92	0

overall SEDs also show signs of enhanced reddening in the nuclear regions (apertures D and E, PA 160).

In order to obtain a more detailed information about the stellar populations we have modelled the spectra extracted from the apertures using the evolutionary synthesis models of González Delgado et al. (2005) and Bruzual & Charlot (2003). These models incorporate high and intermediate spectral resolution stellar libraries. Such resolutions are required to isolate the nebular and the stellar absorption contributions in the spectra of this type of galaxies. To generate these templates we have assumed a Salpeter (1955) initial mass function, instantaneous starburst and solar metallicity (see Tadhunter et al. 2005, for a justification of these assumptions). We then reddened the synthetic spectra using both the Calzetti et al. (2000) reddening law, appropriate for starburst galaxies, and the Seaton (1979) reddening law, representing the Galactic extinction case. Overall, there is good consistency between results obtained with the two reddening laws, demonstrating that the main results are not sensitive to the details of the reddening law assumed, for these optical observations.

To determine the detailed properties of the YSPs we have to fit the whole observed spectrum. We have used two different approaches to perform the fit and determine the best models results. They involve the STARLIGHT[1] (Cid Fernandes et al. 2005) and CONFIT (Robinson et al. 2000; Tadhunter et al. 2005; Holt et al. 2007; Rodríguez Zaurín et al. 2007) codes. The former allows up to 11 stellar components but with the same extinction for all components. On the other hand, the CONFIT approach assumes only two stellar population components of different age, but allows these components to have different reddening. More details of the two techniques are given in Sections 3.1 and 3.2.

Throughout this paper, we define YSPs as stellar components with ages $t_{YSP} \leqslant 0.1$ Gyr, ISPs as stellar components with ages in the range of $0.1 < t_{ISP} \leqslant 2$ Gyr; and old stellar populations (OSPs) as a component with age 12.5 Gyr. Note that we have not used stellar populations with ages in the range of 2 Gyr $< t_{SP} <$ 12.5 Gyr. Generally, for models that include YSPs and ISPs/OSPs, which is the case for both CONFIT and STARLIGHT, it is not possible to distinguish between ages within this range, and therefore we decided not to use such stellar populations during the modelling analysis described below.

3.1 Results from STARLIGHT

STARLIGHT fits simultaneously the continuum points and the absorption lines (high-order Balmer lines, He lines, Ca II H, II K, *G* band, etc.). The program reads an input file that labels the spectral windows that contain emission lines, and these spectral ranges are excluded of the fitting. In these models, we have only used the instantaneous burst single stellar populations (SSPs) from the evolutionary

[1] www.starlight.ufsc.br.

Table 3. Modelling results obtained using the CONFIT code with the Bruzual & Charlot (2003) synthetic SEDs. Column 1: slit PA. Column 2: aperture label. Apertures D and E from PA 160 sample the nuclear regions of the galaxy. Column 3: width of the aperture (the centroid of Ap D is chosen to be the reference point for all the slit positions). Column 4: range of ages for the ISP component. Column 5: range of intrinsic $E(B-V)$ values for the ISP component. Column 6: upper limits for the ages of the YSP component. Column 7: same as Column 5 for the YSP component. Column 8: upper limits for the contribution in flux of the YSP to the model in the normalizing bin (4700–4800 Å), for those cases for which an ISP can model the data with a negligible contribution of a young component.

(1)	(2)	Width of the aperture (arcsec) (3)	Age of ISP (Gyr) (4)	$E(B-V)$ (5)	Age of YSP (Gyr) (6)	$E(B-V)$ (7)	%YSP of total flux (8)
PA 160	Ap A	−12.6 to −8.2	0.6–0.7	0.0–0.2	<0.1	0.0–0.2	<5
	Ap B	−8.2 to −5.4	0.5–0.7	0.0–0.2	<0.1	0.0–0.3	<20
	Ap C	−5.4 to −1.8	0.5–0.7	0.3–0.5	<0.1	0.0–1.0	5–15
	Ap D	−1.8 to 1.8	0.5–0.9	0.0–1.0	<0.08	0.9–1.8	30–63
	Ap E	1.8–4.6	0.5–0.9	0.2–0.6	<0.06	0.9–1.6	22–47
	Ap F	4.6–8.6	0.5–0.7	0.2–0.6	<0.08	0.0–1.5	5–36
	Ap G	8.6–22.6	0.5–0.7	0.0–0.3	<0.07	0.0–0.7	5–20
	AP_{TOTAL}	−24.4 to 28.4	0.5–0.7	0.2–0.6	<0.1	0.0–1.5	5–35
PA 75	Ap A	−26.6 to −8.6	0.5–0.7	0.2–0.5	<0.1	0.0–2.0	<20
	Ap B	−8.6 to −4.2	0.5–0.7	0.2–0.6	<0.1	0.0–1.0	5–25
	Ap C	−4.2 to −1.4	0.5–0.7	0.2–0.6	<0.05	0.0–1.2	5–30
	Ap D	−1.4 to 1.4	0.5–0.7	0.2–0.6	<0.06	0.0–1.5	5–25
	Ap E	1.4–5.0	0.5–0.7	0.2–0.5	<0.05	0.0–2.0	<30
	Ap F	5.0–10.2	0.6–0.9	0.1–0.4	<0.1	0.0–1.2	<25
	Ap G	10.2–34.6	0.7–0.9	0.0–0.3	<0.1	0.0–0.8	<25
	AP_{TOTAL}	−29.4 to 35.8	0.5–0.7	0.2–0.5	<0.1	0.0–1.2	5–25
PA 75*	Ap A	−19.2 to −12.0	0.5–0.7	0.0–0.3	<0.06	0.0–0.6	10–35
	Ap B	−12.0 to 5.2	0.5–0.7	0.0–0.3	<0.1	0.0–1.5	5–25
	Ap C	−5.2 to −2.8	0.5–0.7	0.0–0.3	<0.1	0.0–1.5	<40
	Ap D	−2.8 to 2.8	0.5–0.8	0.0–0.3	0.06	0.0–1.5	<40
	Ap E	2.8–17.6	0.6–0.9	0.0–0.3	<0.06	0.0–1.0	<25
	Ap F	17.6–38.4	0.6–0.9	0.0–0.3	<0.1	0.0–2.0	<15
	AP_{TOTAL}	−23.2 to 45.6	0.5–0.8	0.0–0.3	<0.06	0.0–1.5	5–30

models.[2] The intrinsic extinction is modelled assuming a foreground dust screen, and parametrized by the V-band extinction, A_V. The output is the population vector that represents the fractional contribution of each SSP of a given age and metallicity to the model flux at a given wavelength. The fit is carried out with a simulated annealing plus Metropolis scheme (Cid Fernandes et al. 2005), which searches for the minimum χ^2 between the observations and the combined models.

For this work we used 11 SSPs, corresponding to ages 4, 5, 10, 25, 40, 100, 280, 500, 890 Myr, and 1.25 and 14 Gyr from models by González Delgado et al. (2005). We use solar metallicity, and the Calzetti et al. (2000) extinction law. The results obtained are shown in Table 2 and are summarized as follows.

(i) OSP contribute very little to the optical continuum. Only a few per cent of the flux at 4020 Å is due to stellar populations older than 2 Gyr.

(ii) ISPs with ages in the range of 0.5 Gyr $\leqslant t_{ISP} \leqslant$ 0.9 Gyr account for $\gtrsim$70 per cent of the optical continuum in all apertures apart from apertures D and E in PA 160, sampling the nucleus of the galaxy.

(iii) The contribution of YSPs ($\leqslant$100 Myr) is significant ($\gtrsim$30 per cent) in the nuclear regions.

[2] STARLIGHT can also add a power law to the SSP to fit the continuum, but these models do not consider any contribution by a power law.

(iv) While low intrinsic reddening is found in the extended regions ($0.0 \leqslant E(B-V) \leqslant 0.4$), large intrinsic reddening, $E(B-V) \sim 0.7$–0.8 is required towards the centre of the galaxy.

(v) The modelling results found for the three large apertures are consistent with those of the smaller ones and with each other, as shown in the table.

Similar conclusions are obtained if we use Bruzual & Charlot (2003) synthetic SEDs.

A drawback of the STARLIGHT code is that all stellar population components have the same reddening. Therefore, we have also used the CONFIT code, allowing the two stellar components used in this approach to have different reddenings.

3.2 Results from CONFIT

The CONFIT approach consists of a direct fit of the overall continuum shape of the extracted spectra using on a minimum χ^2 technique (Tadhunter et al. 2005; Rodríguez Zaurín et al. 2007). CONFIT is based on a 'simplest model' approach, i.e. we fit the minimum number of stellar components required to adequately model the data. The main advantage of this approach is that it allows a wide range of reddening values for each of the components to be explored. For this work we have used different combinations of two stellar components (ISP + YSP) with a range of reddening for each component. For each spectroscopic aperture the continuum flux was measured in

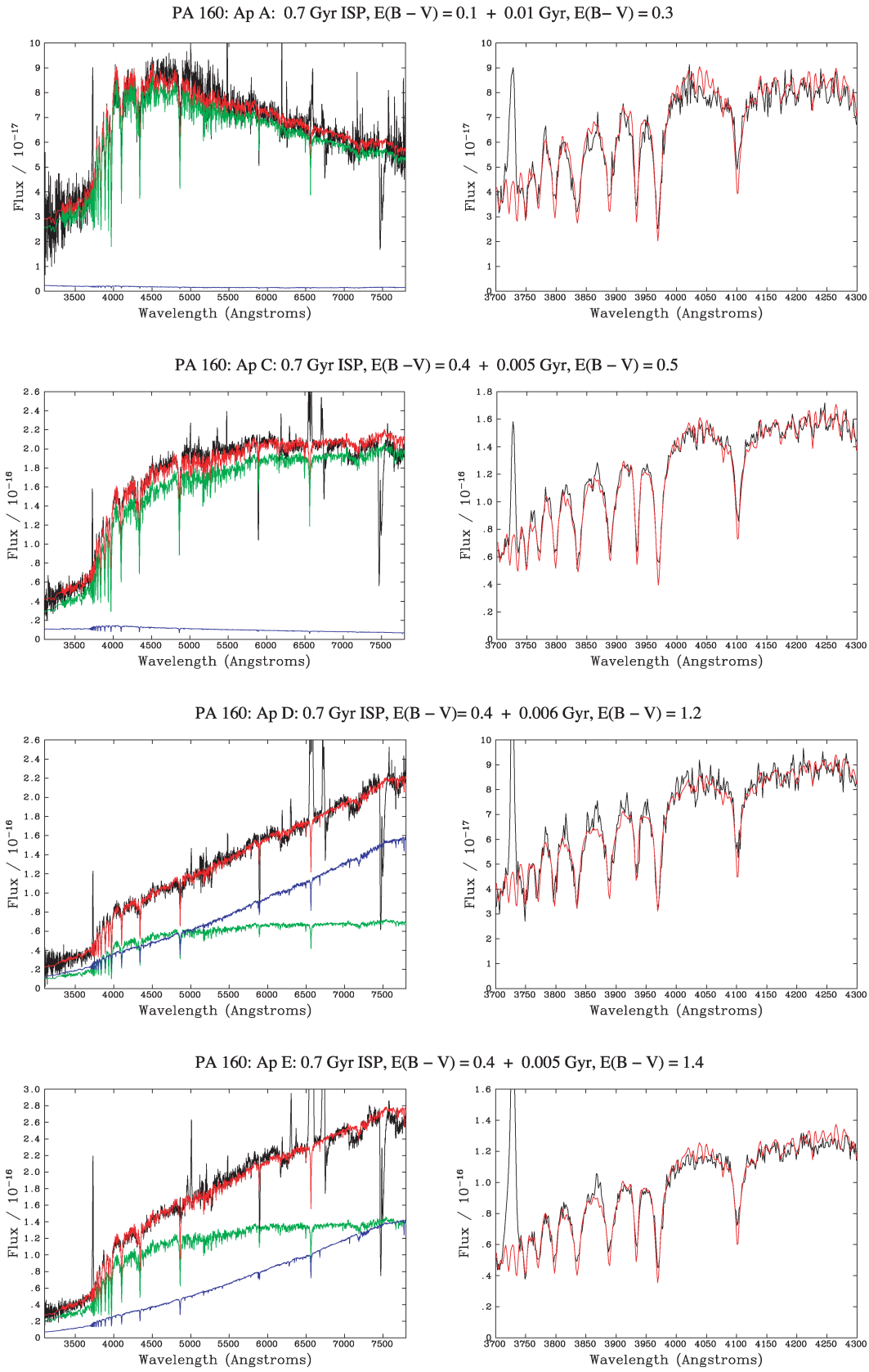

Figure 4. Detailed fits to the spectra extracted for some of the apertures sampling the different regions of the galaxy (see Fig. 1 for the location of the extraction apertures). The green and blue lines are the ISP and YSP components, respectively, while the red lines are the sum of both. It is clear from the figure that a variety of reddenings is required to fit the data for the different apertures. Also shown in the figure are detailed fits of the wavelength range 3700–4300 Å (plots in the right-hand column). The fluxes are presented in wavelength units.

PA 160: Ap F: 0.5 Gyr ISP, E(B – V) = 0.4 + 0.005 Gyr, E(B – V) = 0.5

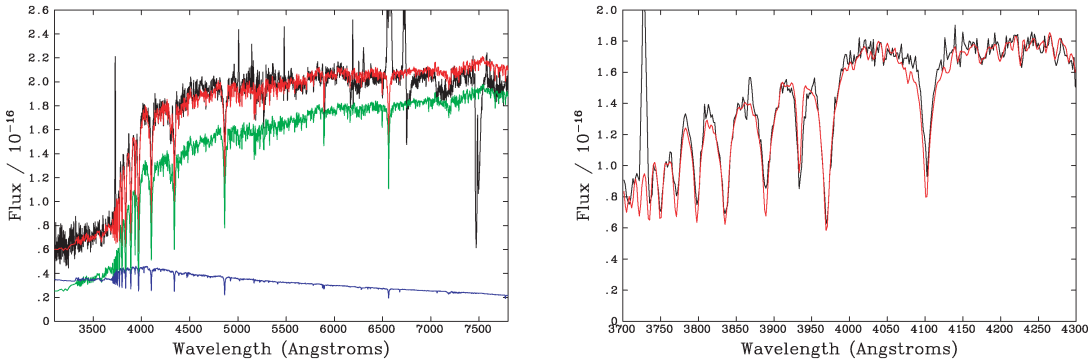

PA 75: Ap A: 0.7 Gyr ISP, E(B –V) = 0.2. + 0.005 Gyr, E(B – V) = 1.0

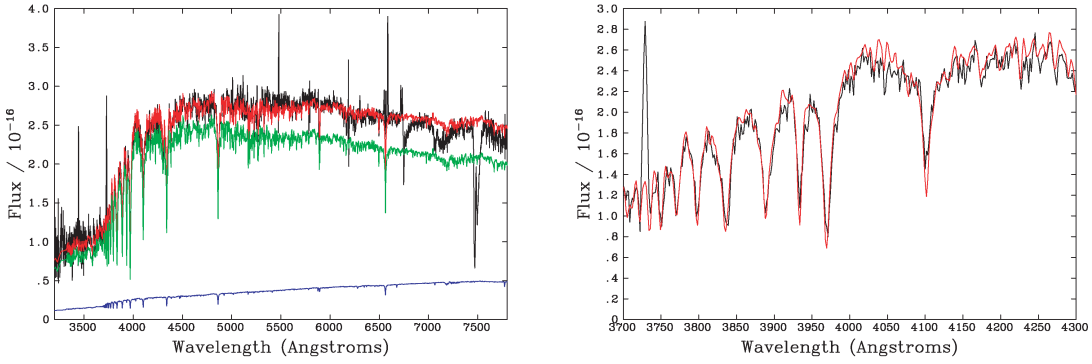

PA 75: Ap G: 0.9 Gyr ISP, E(B – V) = 0.2 + 0.02 Gyr, E(B – V) = 0.2

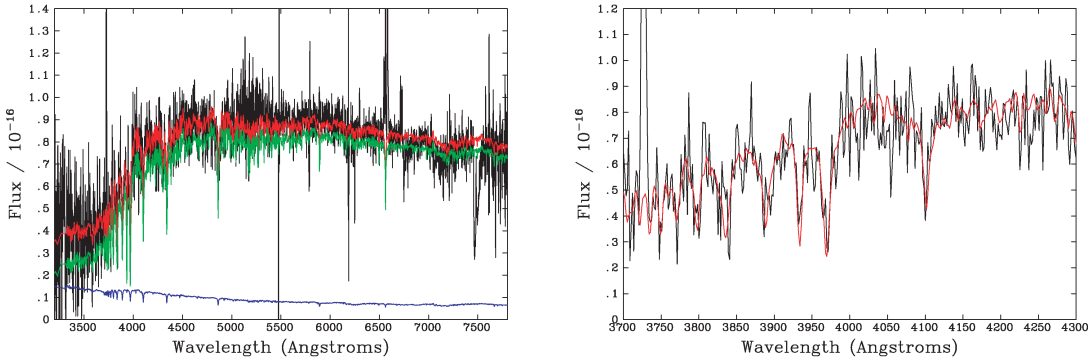

PA 75*: Ap TOTAL: 0.7 Gyr ISP, E(B – V) = 0.2 + 0.01 Gyr, E(B – V) = 0.3

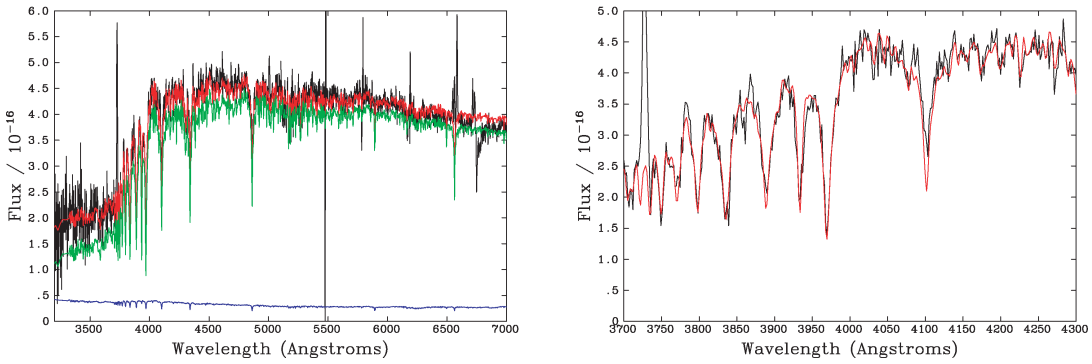

Figure 4 – *continued*

several wavelength bins (∼70) chosen to be as evenly distributed in wavelength as possible, and to avoid strong emission lines and atmospheric absorption features.[3] The model fit results are quantified in terms of the percentage contribution of the different stellar components in a normalizing bin defined as 4700–4800 Å. Due to the uncertainties associated with the flux calibration, as well as the synthetic templates themselves, it is not correct to constrain the total flux in the normalizing bin to be exactly the integrated flux of the observed spectrum in the bin. Therefore the CONFIT code allows the model flux in the normalizing bin to vary up to 125 per cent of the measured flux in that bin.

Potentially adequate fits to the SEDs (reduced $x^2 \leqslant 1.0$) can be obtained for combinations with either small contributions of highly reddened YSPs plus an OSP, or an ISP of low reddening that dominates the spectrum with relatively small contributions from OSP and YSP components (i.e. the age/reddening degeneracy problem). To break this degeneracy we have examined detailed fits to the spectra, considering as valid those models that fit the important absorption features of the spectra adequately (e.g. Ca II K, *G*-band, higher order Balmer lines: see González Delgado, Heckman & Leitherer 2001; Holt, Tadhunter & Morganti 2003; Rodríguez Zaurín et al. 2007).

Table 3 summarizes the results obtained with the CONFIT code. Adequate fits for all 23 apertures extracted from the three slit positions are found with models combining two stellar components, an ISP and a YSP, with no need for an OSP. Fig. 4 shows example fits for apertures selected with the aim of sampling a range of regions in the galaxy. Note that apertures Ap D and E for PA 160 sample the central 2.5 kpc diameter region, corresponding to the dust lanes in the *HST* images. It is clear from the figure that the spectra extracted for these apertures are highly reddened. As well as the best-fitting models, detailed fits in the region of the Balmer lines (3700–4300 Å) are also shown in Fig. 4.

Overall, the results reveal a remarkable uniformity in the estimated stellar ages, with an ISP (0.5 Gyr $\leqslant t_{\rm ISP} \leqslant$ 0.9 Gyr) dominating the optical emission in all apertures, and a YSP ($\leqslant$0.1 Gyr) making a relatively small contribution ($\leqslant$40 per cent) in most apertures. However, note that in the central 2.5 kpc of the galaxy (Ap D and E, PA 160), adequate fits are only found for combinations with a significant contribution from a YSP component (22–63 per cent). In terms of reddening, while the results found in the extended regions are consistent with low intrinsic reddening, one or both stellar components must be highly reddened in the central 5 kpc of the galaxy, clearly indicating high concentrations of gas and dust in the nuclear regions.

At this stage, it is important to add a caveat about the spatial extent of the YSP component. In some of the extended regions of the galaxy (Ap E and F, PA 75*; Ap A, F and G PA 75; Ap A, PA 160), good fits are obtained with a minimal contribution of a YSP template. This is consistent with the STARLIGHT results, where the ISP contribution found for these apertures is $\gtrsim$90 per cent of the total flux. On the other hand, a YSP component is always required to model the data for the apertures sampling the centre of the galaxy. Therefore, while the presence of a YSP in the extended regions remains uncertain, the presence of such a component in the galactic centre is essential. This result is consistent with the age of 10–100 Myr (Mundell et al. 2001) estimated for the duration of the starburst associated with the galactic superwind (Heckman et al. 1996) in the central region of the galaxy, and also with the merger simulations predictions (Barnes & Hernquist 1996; Mihos & Hernquist 1996; Springel et al. 2005) for starbursts characteristic of the final stages of major gas-rich mergers.

Again, the results for the three large apertures show remarkable consistency, both with each other, and with the smaller aperture results presented in the tables.

Overall, the results obtained with CONFIT are broadly consistent with those of STARLIGHT approach, and clearly reinforce the idea that an ISP dominates the optical emission in Arp220.

3.3 The hidden starburst

Our analysis has so far concentrated on the optically visible star formation. It is interesting to consider whether this represents the full extent of star formation in Arp220.

Previous studies based on radio observations (Smith et al. 1998) or the galactic superwind (Heckman et al. 1996; Mundell et al. 2001), have found star formation rates (SFR) up to $100\,{\rm M}_{\odot}\,{\rm yr}^{-1}$ for Arp220. An independent estimate of the SFR can be obtained using the published flux of the Brα line, $F({\rm Br}\alpha) = 1.8 \times 10^{-13}\,{\rm erg\,s^{-1}\,cm^{-2}}$ (Genzel et al. 1998). Using the IR extinction laws of Indebetouw et al. (2005) and Rieke & Lebofsky (1985) along with the estimated visual extinction for the nuclear region of Arp220 ($A_{\rm v} \sim 45$ mag, Sturm et al. 1996; Genzel et al. 1998), we derive a Brα luminosity of $L({\rm Br}\alpha) = 9.2 \times 10^{41}\,{\rm erg\,s^{-1}}$. Assuming Case B recombination theory we then derive an Hα luminosity of $L({\rm H}\alpha) = 3.3 \times 10^{43}\,{\rm erg\,s^{-1}}$. It is now straightforward to estimate the SFR in the galaxy using the relationship between Hα luminosity and SFR given by Kennicutt (1998). We find a SFR of $\sim$260 $\rm M_{\odot}\,yr^{-1}$, enough to power the entire mid- to far-IR luminosity observed in Arp220. Moreover, the absence of mid-IR, high-ionization emission lines ([Ne V]λ14.322 μm, [O IV]λ25.890 μm. Genzel et al. 1998) suggests no hidden AGN activity, reinforcing the idea that starburst activity powers the mid-to-far-IR luminosity of the source. In such a case, it is also possible to measure the SFR of the galaxy using the IR luminosity (Kennicutt 1998). For a value of $L_{\rm IR} = 1.3 \times 10^{12}\,{\rm L}_{\odot}$ for Arp220 (Soifer et al. 1987) we obtain a SFR $= 224\,{\rm M}_{\odot}\,{\rm yr}^{-1}$, which is remarkably consistent with the value found using the Brα flux.

However, there is no clear evidence for the presence of ongoing star formation activity at optical wavelengths, based on H II region-like optical emission line ratios (Veilleux et al. 1999). In order to measure the bolometric luminosity associated with the visible stellar populations detected in the optical, we added the spectra extracted for all the apertures of the region limited by the dashed-line box in Fig. 1. Since our spectroscopic slits used do not cover the entire extent of the central region, a large aperture chosen to match the extent of the box was extracted from an *HST* ACS (F435W) image (HST proposal 9396, PI C. Wilson). We then scaled the combined spectrum to match the flux measured from the aperture, in order to account for possible flux losses. Assuming an ISP + YSP combination consistent with the modelling results of section 3.2[4] and correcting for reddening effects, we determined the bolometric luminosity of all the components in the scaled spectrum and added them, obtaining a total bolometric luminosity $L_{\rm bol} \sim 1.6 \times 10^{11}\,{\rm L}_{\odot}$.

[3] Note that it is a further difference with the STARLIGHT code which fits every pixel apart from regions (e.g. those containing emission lines or atmospheric emission features) that are specifically masked out.

[4] ISP of 700 Myr [$E(B-V) = 0.2$] + a YSP of 5 Myr [$E(B-V) = 0.5$] making a contribution of 80 per cent and 20 per cent of the total flux, respectively.

This is an order of magnitude less than the mid- to far-IR luminosity of the source. Therefore, especially considering that not all the optical emission is absorbed by dust, it is clear that the stellar populations detected at optical wavelengths cannot power the far-IR luminosity of the source; most of the ongoing star formation in the nuclear regions is hidden by dust.

3.4 Summary of the key results

To summarize the main results, the modelling of our spectra provides evidence for three stellar populations in Arp220.

(i) Dominant ISP: we have found an ISP, of ages 0.5 Gyr $\leqslant t_{\rm ISP} \leqslant 0.9$ Gyr, that dominates the optical spectrum, extending across 65 arcsec ($\sim$24 kpc), and covering the measurable extent of the galaxy.

(ii) YSP component: we have found a young stellar component, of age $t_{\rm YSP} \leqslant 100$ Myr, with varying contributions across the galaxy, but particularly significant in the nuclear regions, where it is highly reddened.

(iii) Hidden starburst: our results reinforce the idea that there is prodigious ongoing star formation activity that is hidden at optical wavelengths. This is likely to be related to the radio supernovae detected in the centre of the galaxy (Smith et al. 1998), as well as the powerful mid to far-IR emission from this object.

4 DISCUSSION

4.1 Comparison with previous results

Wilson et al. (2006) found evidence for a centrally located YSP ($\leqslant$10 Myr) and an intermediate-age ($\sim$300 Myr) stellar population spread towards the north of the galaxy in their photometric study of the cluster populations in Arp220. These results are broadly consistent with the results presented in this paper. In addition, we find evidence for ISPs at all locations in the galaxy.

There have been relatively few attempts in the past to study the stellar populations in the diffuse light of ULIRGs. Canalizo & Stockton (2000a,b, 2001) found stellar ages ranging from currently ongoing starburst activity to post-starburst ages of $\lesssim$300 Myr in their sample of 'transition QSOs' – objects that may represent a transitionary stage between ULIRGs and QSO. In contrast, the ages found for the dominant stellar populations in Arp220 are generally older than 300 Myr. Note, however, that Canalizo & Stockton (2000a,b, 2001) used only one stellar component for their modelling.

More recently, Rodríguez Zaurín et al. (2007) applied the same techniques used here to the ULIRG/radio galaxy PKS1345+12. Overall, the results found in their paper are consistent with the results found here for Arp220, with a mixture of YSP and ISP components. However, precise age determination for the ISP component is more difficult in PKS1345+12 because of the presence of a strong OSP component.

We are currently analysing the optical spectra of a sample of 40 ULIRGs (Rodriguez et al., in preparation). We find that the modelling results are consistent with a combination of YSP + ISP components for the majority of the objects in our sample. However, the YSPs found in these galaxies make a larger contribution than in the case of Arp220, and sometimes dominate the optical spectra. Finally, similar results in terms of the mix of stellar populations have recently been obtained in detailed spectroscopic studies of LIRGs (González Delgado 2007).

4.2 The origin of the ISPs

In order to use studies of the stellar populations to investigate star-forming histories in major galaxy merges it is important to understand the extent to which the stellar populations have been formed during the merger. A potential issue is contamination by the YSPs present in the galaxy discs prior to the star of the merger. As a first approach to investigate the origin of the ISPs we used the CONFIT code and combined unreddened Sa, Sb and Sc galaxy template spectra (Kinney et al. 1996) with a stellar population with ages in the range $0.001 \leqslant$ age $\leqslant 2$ Gyr and reddenings $0.0 \leqslant E(B-V) \leqslant 2.0$.

No good fits were found for combinations of Sa, Sb or Sc galaxy templates without a significant additional contribution of a YSP or an ISP component. However, the Kinney et al. (1996) templates represent an average for several galaxies of the same morphological type, and each type encompasses a range of individual galaxy spectra, some of which deviate substantially from the averaged SED. Therefore, although the modelling results obtained using this combination suggest that the stellar populations detected in the optical for the ULIRG Arp220 have been formed during the merger event rather than captured, we cannot entirely rule out the idea that the ISPs detected in the galaxy represent the disrupted discs of one or more of the merging galaxies.

Another way to address this issue is to compare the mass of YSPs in late-type spiral galaxies, the likely progenitor galaxies, with the values found here for the ISPs in Arp220. The reason to focus only on YSPs in the parent galaxies is that, if the star formation in the discs is truncated during the merger, these are the populations which may evolve into ISPs detected today in Arp220. Since our three slit positions do not cover the full extent of the object, we used the apparent magnitude of the galaxy in the V band, $m_V = 13.2$ (Taylor et al. 2005), and applied the same techniques described in section 3.4 to account for possible slit losses. We obtain total masses in the range 2.7×10^{10}– $4.3 \times 10^{10}\,{\rm M}_{\odot}$ for the ISPs in Arp220. To estimate the stellar mass content of late-type spiral galaxies, we modelled a Sc galaxy template (Kinney et al. 1996) combining a 12.5 Gyr OSP with a YSP. We find that we can model the template with an OSP plus YSPs of age $t_{\rm YSP} \leqslant 20$ Myr contributing 70–100 per cent of the total flux in the normalizing bin (4420–4500 Å, chosen to be close to the B-band wavelength range). We then assumed the same values for the contribution of each component to the median B-band monochromatic luminosities of Sc galaxies (Roberts & Haynes 1994). Since the templates are generated for $1\,{\rm M}_{\odot}$, by scaling we were able to estimate the total mass and the mass contribution of each of the components. We estimated a range of $3.6 \times 10^{9} - 3.7 \times 10^{11}\,{\rm M}_{\odot}$ for the total stellar mass of the population of typical Sc galaxies in the large compilation of Roberts & Haynes (1994), of which only 1.2×10^{9}– $8.5 \times 10^{9}\,{\rm M}_{\odot}$ is accounted for the YSP component. Therefore, it is possible that the ISPs detected in Arp220 represent the captured discs of one or more of the parent galaxies, but only if these galaxies are among the most massive late-type spirals.

In terms of gas content, Scoville et al. (1997) found an H_2 mass of $\sim 3 \times 10^{10}\,{\rm M}_{\odot}$ for Arp220. However, they used a standard Galactic CO-to-H_2 ratio, which is likely to overestimate the molecular gas mass M(H_2) by a factor of 3 (Solomon et al. 1997). On the other hand, an upper limit for the H I mass value for Arp220 is $5.0 \times 10^{9}\,{\rm M}_{\odot}$ (Mirabel & Sanders 1988). Therefore, the total gas mass in the galaxy, M(H_2 + H I), is of the order of $\sim 1.5 \times 10^{10}\,{\rm M}_{\odot}$. In comparison, the median value of the H I mass content of Sc galaxies is $0.8 \times 10^{10}\,{\rm M}_{\odot}$ (Roberts & Haynes 1994). Assuming a typical H_2/H I mass ratio of 0.7 (Young & Knezek 1989)

for such galaxies, we find a gas mass content of $M(H_2 + H\,I) \sim 1.4 \times 10^{10}\,M_\odot$ for a typical Sc galaxy. Therefore, we conclude that it is possible for a merger of two typical spiral galaxies to account for the gas content estimated in Arp220 provided that a large fraction of the gas is not ejected during the merger (Di Matteo et al. 2007) or transformed into stars. However, if a substantial proportion of the ISPs are formed in the merger, then the total amount of gas required is much larger, implying a merger between two Sc galaxies in the upper 25 per cent of the H I mass range (Roberts & Haynes 1994).

4.3 Comparison with models

Arp220 is a double nucleus system with a separation of 0.95 arcsec, corresponding to ∼345 pc, that exhibits tidal tails in the optical. The morphology of the galaxy suggests that it is in the final stages of the merger event, just before the two nuclei coalesce. In this section we will compare the results found in this paper with the prediction of the models for the star formation activity at such a stage of a merger event.

In general, simulations predict two epochs of starburst activity (Barnes & Hernquist 1996; Mihos & Hernquist 1996; Springel et al. 2005) in major gas-rich mergers: the first occurring just after the first encounter, and the second, more intense, episode towards the end of the merger, when the nuclei coalesce. However, both the time lag and the relative intensity of the peaks of starburst activity during the merger event depend on several factors: the presence of bulges, feedback effects, gas content and orbital geometry. For example, the presence of a bulge acts as a stabilizer of the gas against inflows and formation of bar structures, allowing stronger starburst activity towards the end of the merger event (Barnes & Hernquist 1996; Mihos & Hernquist 1996). On the other hand, AGN feedback effects (e.g. quasar-driven winds) disrupt the gas surrounding the black hole, acting against the star formation activity (Springel et al. 2005).

In the case of Arp220, we derive SFRs of $\sim 260\,M_\odot\,yr^{-1}$, consistent with a starburst being responsible for the IR luminosity of the galaxy (Genzel et al. 1998). Based on the results of the simulations (Springel et al. 2005), highly gas-rich disc galaxies must be involved in the merger event to account for such high SFRs. In this context, the results found in the previous section are consistent with the model predictions. It is possible that the dominant ISPs detected in Arp220 are associated with the first enhancement in star formation activity that occurs in the early stages of the merger, coinciding with the first encounter between the merging nuclei. However, because of the potential contamination from stars in the disrupted discs of the merging galaxies (section 4.2), the fraction of ISPs formed in the merger is not known with any accuracy. On the other hand, the YSPs detected in the centre of the galaxy, as well as the ULIRG activity, are likely to be related to the major enhancement of the activity as the two nuclei coalesce in the final stages of the merger. It is notable that the ages of the YSP ($t_{YSP} < 0.1$ Gyr) are consistent with the 0.1 Gyr time-scale of the final starburst predicted by the merger simulations.

5 CONCLUSIONS

The results presented in this paper demonstrate the utility of spectroscopic studies of the diffuse light for investigating the evolution of the stellar populations in ULIRGs.

We have found evidence for a complex star formation history in the ULIRG Arp220, with at least two distinct episodes of starburst activity. The results are consistent with an ISP of age $0.5 \leqslant t_{ISP} \leqslant 0.9$ Gyr, dominating the optical emission throughout the body of the galaxy. We have also detected YSPs ($\leqslant$100 Myr) located in the central ∼2.5 kpc that contribute significantly to the optical emission. This latter population is likely to be related to the last enhancement of the activity towards the end of the merger event.

On the other hand, we have estimated that the bolometric luminosity accounted by the optically visible stellar populations and compared it with the IR luminosity of the galaxy. We conclude that we are not directly detecting the bulk of the starburst activity responsible for the ULIRG phenomenon in Arp220, which is likely to be related to the radio supernovae found by Smith et al. (1998), representing another 'extra' episode of star formation activity apart from the two suggested by our modelling results. It is clear that our results for Arp220 are consistent with the emerging evidence for a complex and multimodal star formation activity in merging systems (The Antennae: Whitmore et al. 1999, NGC 7252: Maraston et al. 2001, PKS1345+12: Rodríguez Zaurín et al. 2007).

In terms of reddening, while the presence of highly reddened stellar components is unlikely in the extended regions of the galaxy, high reddening values are required to match the data for the apertures sampling the nuclear regions, coinciding with dust lanes in the *HST* images. Our results show the importance of accounting for reddening when modelling the stellar populations in star-forming galaxies.

Finally, we note that the modelling results for the three large apertures, representing the integrated light of the galaxy, are consistent with those of the detailed study based on smaller apertures. This gives confidence to studies of ULIRGs at medium and high redshifts, suggesting that age measurements based on relatively large aperture studies of the diffuse light at such redshifts, are representative of the stellar populations of the galaxies as a whole.

ACKNOWLEDGMENTS

JRZ acknowledges financial support in the term of a PPARC studentship. RMGD is supported by the Spanish grant AYA2004-02703. The WHT is operated on the island of La Palma by the Isaac Newton Group in the Spanish Observatorio del Roque de los Muchachos of the Instituto de Astrofisica de Canarias. We thank Paul Crowther for useful discussions and Roberto Cid for STARLIGHT. We also thank the referee for her useful comments which have helped to improve the manuscript.

REFERENCES

Barnes J., Hernquist L., 1996, ApJ, 471, 115
Bruzual G., Charlot S., 2003, MNRAS, 344, 1000
Calzetti D., Armus L., Bohlin R., Kinney A., Koornneef J., Storchi-Bergman T., 2000, ApJ, 533, 682
Canalizo G., Stockton A., 2000a, AJ, 528, 201
Canalizo G., Stockton A., 2000b, AJ, 120, 1750
Canalizo G., Stockton A., 2001, ApJ, 555, 719
Cid Fernandes R., Mateus A., Sodré L., Stasinska G., Gomes J., 2005, MNRAS, 358, 363
Di Matteo P., Combes F., Melchior A.-L., Semelin B., 2007, A&A, 468, 61
Genzel R. et al., 1998, ApJ, 498, 579
González Delgado R., 2007, in Knapen J., Mahoney T., Vazdekis A., eds, Pathways Through an Eclectic Universe. Astron. Soc. Pac., San Francisco, in press
González Delgado R., Heckman T., Leitherer C., 2001, ApJ, 546, 845

González Delgado R., Cerviño M., Martins L. P., Leitherer C., Hauschildt P., 2005, MNRAS, 357, 945
Graham J., Carico D., Matthews K., Neugebauer G., Soifer B., Wilson T., 1990, ApJ, 354, L5
Heckman T., Dahlem M., Eales S., Fabbiano G., Weaver K., 1996, ApJ, 457, 616
Holt J., Tadhunter C. N., Morganti R., 2003, MNRAS, 342, 227
Holt J., Tadhunter C., González Delgado R., Inskip K., Rodríguez Zaurin J., Emonts B., Morganti R., Wills K., 2007, MNRAS, 381, 611
Houck J. et al., 1984, ApJ, 278, L63
Houck J., Sneider D., Danielson G., Beichman C., Lonsdale C., Neugebauer C. B. T. S., 1985, ApJ, 290, L5
Indebetouw R. et al., 2005, ApJ, 619, 931
Joseph R., Wright G., 1985, MNRAS, 214, 87
Kennicutt R., 1998, ARA&A, 36, 189
Kinney A., Calzetti D., Bohlin R. C., McQuade K., Storchi-Bergmann T., Schmitt H. R., 1996, ApJ, 467, 38
Le Floc'h E. et al., 2005, ApJ, 632, 169
Lutz D., Veilluex S., Genzel R., 1999, ApJ, 517, L13
Maraston C., Kissler-Patig M., Brodie J., Bramby P., Huchra J., 2001, A&A, 370, 116
Mihos J., Hernquist L., 1996, ApJ, 464, 641
Mirabel I., Sanders D., 1988, ApJ, 355, 104
Mundell C., Ferruit P., Pedlar A., 2001, ApJ, 560, 168
Osterbrock D., Fulbright J., Keane M., Trager S., 1996, PASP, 108, 277
Rieke G., Lebofsky M., 1985, ApJ, 288, 618
Roberts M., Haynes M., 1994, ARA&A, 32, 115
Robinson T., Tadhunter C., Axon D., Robinson A., 2000, MNRAS, 317, 922
Rodríguez Zaurín J., Holt J., Tadhunter C., González Delgado R., 2007, MNRAS, 375, 1133
Salpeter E., 1955, ApJ, 121, 161
Sanders D. B., Mirabel I. F., 1996, ARA&A, 34, 749
Schlegel J., Finkbeiner D., Davis M., 1998, ApJ, 500, 525
Scoville N., Yun M., Bryant P., 1997, ApJ, 484, 702
Scoville N. et al., 1998, ApJ, 492, L107
Seaton M., 1979, MNRAS, 187, 73
Smith H., Lonsdale C., Lonsdale C., Diamond P., 1998, ApJ, 493, L7
Soifer B. et al., 1984a, ApJ, 278, L71
Soifer B. et al., 1984b, ApJ, 283, L1
Soifer B., Sanders D., Madore B., Neugebauer C., Danielson G., Elias E., Lonsdale C., Rice W., 1987, ApJ, 320, 74
Solomon P., Downes D., Radford S., Barret J., 1997, ApJ, 478, 144
Springel V., Di Mateo T., Hernquist L., 2005, MNRAS, 361, 776
Sturm E. et al., 1996, A&A, 315, L133
Surace J. A., Sanders D. C., 1999, ApJ, 512, 162
Tadhunter C. N., Robinson T. G., González Delgado R. M., Wills K., Morganti R., 2005, MNRAS, 356, 480
Taylor V., Jansen R., Windhorst R., Odewahn S., Hibbard J., 2005, ApJ, 630, 784
Veilleux S., Sanders D. B., Kim D. C., 1999, ApJ, 522, 139
Whitmore B., Zhang Q., Leitherer C., Fall S., Schweizer F., Miller B., 1999, AJ, 118, 1551
Wilson C., Harris W., Longden R., Scoville N., 2006, ApJ, 641, 763
Young J., Knezek P., 1989, ApJ, 347, L55

This paper has been typeset from a TEX/LATEX file prepared by the author.